International Journal of Latest Trends in Engineering and Technology
Special Issue AFTMME-2017, pp. 037-045
e-ISSN:2278-621X

CONTRIBUTION OF VARIOUS COATING TECHNIQUES IN THE FIELD OF MICROWAVE ABSORPTION – A REVIEW

Gagan Deep Aul[1], Vikas Chawla[2] & Santosh K Vishvakarma[3]

Abstract- Surface coating techniques are basically known for enhancing the mechanical, physical characteristics of the target (substrate) whereas it is very interesting to explore the significant involvement of these techniques to impart absorption to incident electromagnetic signals. This characteristic of the coating is very helpful not only in the field of defense (reduction of radar signature of aircraft, ships, tanks, and targets) but for various civil applications as well. Specially coating techniques are helpful in development of stealth aircrafts as it facilitate to design anti radar aircrafts without modifying the aerodynamic structure/design, because it is a very cumbersome for the design engineers to overcome the trade-offs between the aerodynamics and stealth properties of the air craft. In this paper different coating techniques used for microwave absorption has been studied to elaborate their pros and cons.
Keywords: Electromagnetic, Absorption, Atmospheric Plasma Spraying, Flame Spraying, HVOF, Coatings, Stealth

1. INTRODUCTION

Absorbers in the RF/microwave realm are materials that attenuate the energy in an electromagnetic wave. Absorbers are used in a wide range of applications to eliminate stray or unwanted radiation that could interfere with a system's operation. Absorbers can be used externally to reduce the reflection from or transmission to particular objects and can also be used internally to reduce oscillations caused by cavity resonance. They can also be used to recreate a free space environment by eliminating reflections in an anechoic chamber [1]. Absorbers can take many different physical forms including flexible elastomers or foam or rigid epoxy or plastics. They can be made to withstand weather and temperature extremes. Absorbers have become a critical element in some systems to reduce interference between circuit components. Radar absorbing materials (RAMs) is a kind of function materials [2], which can absorb or reduce the echo of the object scatter by transforming the electromagnetic energy [3-6]. It is widely used for multiple applications in domains such as stealth technology, microwave unreflect chamber and bolometer [7-8]. Traditional RAMs such as composite coating for aircraft have narrow absorbing frequency bandwidth. Besides, the bandwidths of reflection loss (RL) are largely dependent on the coating thickness. These finds have been confirmed by many studies on traditional RAMs.

Miriam Floristán et.al experimentally studied coating systems acting as an efficient absorber for 140GHz radiation [0]. Al_2O_3, TiO_2, Cr_2O_3 and ZrO_2 and mixtures of Al_2O_3 & TiO_2 in compositions 87:13
& 50:50 commercially available powders were sprayed on Cu plates (50mm×50mm×2mm) using atmospheric plasma spraying. All the powders had particle size distributions of −20+5µm.
To enhance coating adhesion substrates were degreased using acetone and were grit blasted prior to coating with 250 µm alumina grit, pressure of 0.6MPa at an angle of 90^0 and distance of approximately 200mm. An electric arc is created between an anode and a cathode in the spray torch. A gas mixture is injected and due to its interaction with the electric arc, a plasma jet is generated. The spray powder is melted in the plasma jet and propelled towards the substrate surface. Upon impacting at the surface, the particles deform and rapidly solidify, building up the coating.
By varying coating thickness from 50µm to 250µm, it was found that the microwave absorption of the layers is strongly determined by its thickness and that for each powder the thickness range for an optimal absorption differs as shown in figure 1. The coatings has been carried at four different spray angles i.e. 30^0, 50^0, 70^0 & 90^0 (angle between the center axis of the plasma torch and the surface of the substrate), the influence of lower spray angles to cover all the areas of the complex geometry of practical targets, on the coating microstructure and absorption capability was analyzed and represented in Figure 2 and Figure 3.

[1] Research Scholar, IKGPTU, Jalandhar (Punjab), India
[2] Professor, Mechanical Engineering, IKGPTU, Jalandhar (Punjab), India
[3] Associate Professor, Electrical Engineering, IIT, Indore, India

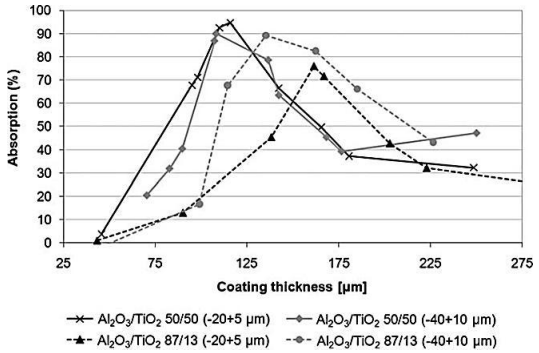

Figure 1: Microwave absorption as a function of the coating thickness.

Low spray angles lead to the formation of more elongated splats orientated in the direction of spraying, as can be seen in Figure 2.

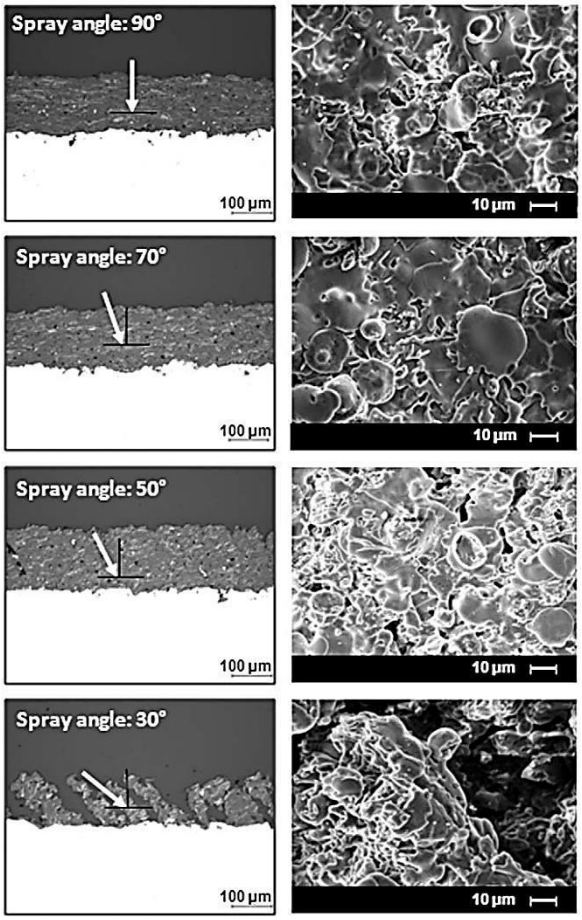

Figure 2: Cross section micrographs and SEM pictures of the coating surfaces deposited.

As a consequence, impinging particles cannot cover some regions that are shadowed in the saw tooth, leading to the formation of pores. Increased coating roughness and low deposition efficiency are also characteristic of off-normal spray angles.

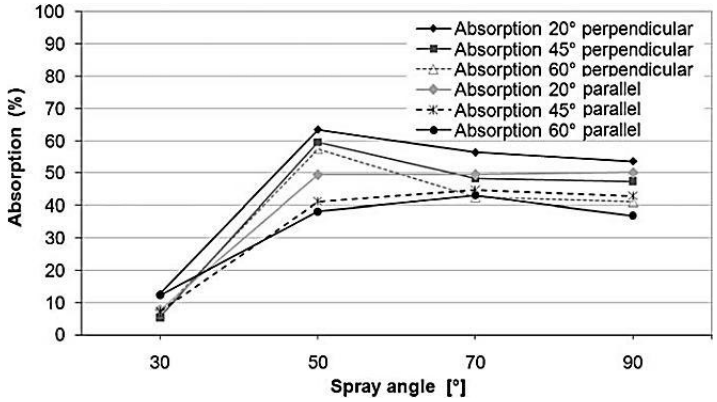

Figure 3: Coating microwave absorption depending on the spray angle.

For microwave absorption all the samples were for measurement with parallel and perpendicular polarization, with incidence angles of 20^0, 45^0 and $60^0$with a fixed thickness of 150µm.

As can be seen in Figure 3, the absorption of the coatings is comparable for samples sprayed with angles between 90^0 and 50^0, and it drops strongly for the spray angle 30^0. This behavior is related to the highly inhomogeneous coating microstructure characterized by high porosity and roughness obtained with low spray angles. Microwave absorption characteristics of Al_2O_3: TiO_2 in different composition and two additional ceramics were tested; Cr_2O_3 and ZrO_2 (Figure 4).

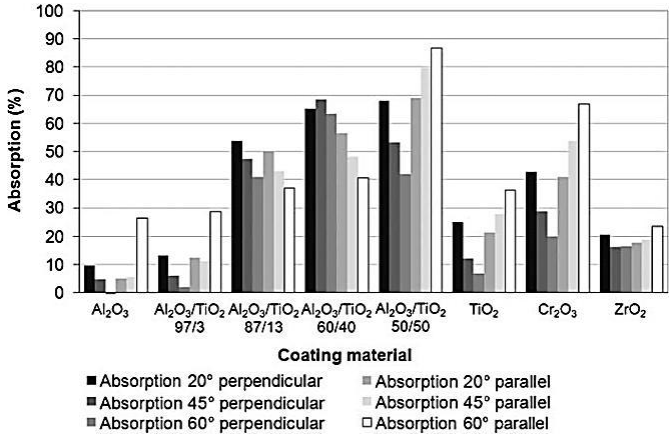

Figure 4: Coating microwave absorption for different sprayed materials.

It was concluded experimentally that coating thickness, angle of coating and composition (Al_2O_3:TiO_2 ratio) strongly influence the absorption characteristics. Using Atmospheric Plasma Spraying (APS), ceramic oxides coated cupper substrate showed maximum absorption up to 75.7% in the case of Al_2O_3/TiO_2 87:13 coatings.

Darja Lisjak et al. discussed experimentally preparation of barium hexaferrite coatings using atmospheric plasma spraying [10]. They indicated that typical commercial absorbers are in the form of ceramics or polymer composites filled with absorbing powders. These absorbers represent a special element in electronic modules and have only a limited possibility to be adjusted to the various shapes of the components that require electromagnetic protection. However, this can be overcome with the application of spraying technologies for the preparation of absorbent coatings. Spraying technologies are well-known methods for the preparation of coatings on various objects that have a range of geometries. Despite this, only a few examples of using spraying for the preparation of electromagnetically active coatings have been reported.

Thick coatings of barium hexaferrite with the compositions $BaFe_{12}O_{19}$ and $BaCoTiFe_{10}O_{19}$ in powder fractions 20−85µm and 20−40µm were prepared using atmospheric plasma spraying (APS) technology. The $BaFe_{12}O_{19}$ powder was sprayed on steel by APS with an F4 torch from Sulzer Metco, using a plasma composed of argon and hydrogen. The hydrogen has a good thermal conductivity and imparts a higher temperature to the plasma. An additional Ba hexaferrite sample was produced with similar plasma parameters, but was sprayed on glass substrate and with a smaller grain size 20–40µm instead of 20–85µm for the first sample. In order to keep temperature as low as possible the sample was prepared on glass without hydrogen and with a lower current than for the Ba hexaferrite sample. The spray parameters are as listed in Table 1.

Table 1 Spraying Parameters

Compo sition	Current	Gas:Ar(SLPM)	Gas:H2 (SLPM)	Carrier gas (SLPM)	Sprayz distance(mm)	Grainsize(µm)	Substrate
BaFe12O19	500	50	6	3.5	130	20–5	Steel
BaFe12O19	500	50	6	3.5	130	20–40	Glass
BaFe10CoTiO19	400	50	0	3.5	130	60–80	Glass

The AS-deposited coatings were annealed at 380– 1300^0 C for up to 3 h in air. It was found out that the Fe from the steel substrate reacts with the coating at 600^0 C and higher thus steal is not a suitable substrate, while the glass substrate proved to be chemically compatible with the coating material. Therefore, the results presented are obtained from the coatings prepared on glass substrates and/or on powdered coatings.

The microstructures of the powders and the phase composition of the coatings and of the coatings' cross-sections were observed with the scanning electron microscope (FEI XL30) combined with energy-dispersive X-ray analyses for the phase compositions as shown in Figure 5

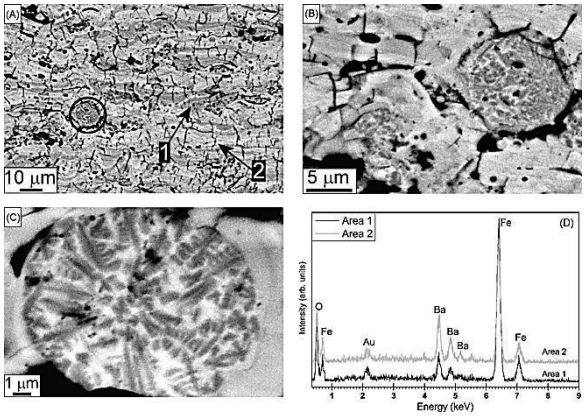

Figure 5: SEM micrograph of the polished cross-section of the as-deposited Ba hexaferrite coating (A – the circle indicates a spherical inclusion), detailed views of two spherical inclusions (B and C) and EDX microanalyses of the regions labelled 1 and 2 in panel A (D).

Finally it was concluded that for glass substrate, APS process does not provide enough time for the recrystallization of $BaFe_{12}O_{19}$. Nevertheless, the formation of the single-phase coatings proves that there was no significant loss of cations during the APS process.

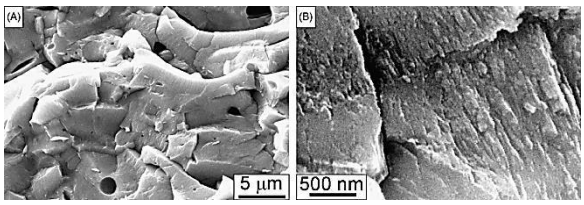

Figure 6: SEM micrographs of the fracture surfaces of the as-deposited M coating at different magnification

The measured electromagnetic properties of the sintered Ba hexaferrite shown that the reflection from the coated metal plate has its minimum when the coating thickness is 0.15–0.25mm at 46 GHz, when only a few percent of the incoming power is reflected backwards. Whereas Ba-CoTi hexaferrite ceramic samples shows the reflection from the coated metal plate has a minimum when the coating thickness is 1– 4mm at a frequency range 3–9 GHz, when less than 10% of the incoming power is reflected backwards.

M. Bégard et al. explored Co,Ti-substituted Ba-hexaferrite ($BaCoTiFe_{10}O_{19}$) coatings for applications as microwave absorbers were deposited by the APS and HVOF techniques, using $BaCoTiFe_{10}O_{19}$ powders manufactured by solid-state reaction followed by spray-drying [11]. The powder feedstock, with composition $BaCoTiFe_{10}O_{19}$, was synthesized by solid-state reaction from $BaCO_3$ (Merck, 98.5% pure), Co_3O_4 (Alfa Aesar, 99% pure), TiO2 (Alfa Aesar, Anatase 99% pure) and Fe2O3 (NK-α SEW, 99.65% pure) in 1–2 kg batches. Spherical agglomerates having various size distributions were thus produced and employed for the spraying experiments.

Table 2 Hvof Deposition Parameters.

Sample label	HVOF-1	HVOF-2	HVOF-3
Torch model	HV2000	HV2000	DJ Hybrid
Fuel type and flow rate (Sl/min)	Propane	Propane	H2
	62	69	600
Oxygen flow rate (Sl/min)	285	278	245
Stand-off distance (mm)	200	200	200
Particle size (μm)	12–30	12–30	12–30

The agglomerated powders were sprayed by high velocity oxygen fuel (HVOF) flame-spraying and by atmospheric plasma spraying (APS). Specifically, three different parameter sets were employed for HVOF-spraying (labelled as HVOF-1, HVOF-2 and HVOF-3 in Table 2), whereas six different parameter sets were initially chosen for APS (Table 3: APS-1 to APS-6). Based on the results which will be presented in the following sections, two more APS coatings were produced, labelled as APS-7 and APS-8 (Table 3), respectively.

Table 3 Aps Deposition Parameters

Sample	Current (A)	Ar (Sl/min)	H2 (Sl/min)	Carr gas (Sl/min)	Spray dist. (mm)	Inj. Dia. (mm)	Part. size (μm)
APS-1	500	40	6	3.5	130	1.8	60–80
APS-2	500	40	6	3.5	130	1.8	20–40
APS-3	500	50	6	3.5	130	1.8	60–80
APS-4	400	40	6	3.5	130	1.8	20–40
APS-5	500	40	4	3.5	130	1.8	60–80
APS-6	500	40	6	3.5	100	1.8	20–40
APS-7	400	50	0	3.5	130	1.8	60–80
APS-8	400	50	0	3.5	130	1.8	36–80

All of the coatings were deposited onto a glass-ceramic substrate, chosen because of its non-magnetic characteristics, which make it suitable for the measurement of the magnetic properties of the coatings.

All of the HVOF-sprayed coatings, regardless of the deposition parameters, did not retain the crystalline structure of the Ba-hexaferrite compound; indeed, results in very poor magnetic properties: in all cases, the saturation magnetization of these coatings, measured by the VSM technique under a maximum applied field of 1 T (M1 T), is about 3 emu/g, whereas literature values for the saturation.

APS-1 to APS-6 coatings were produced, aiming to investigate the effects of the systematic variation of some important deposition parameters (Ar and H2 flowrates, arc current, spray distance, particle size distribution) on the coatings' properties Some weak peaks of the Ba-hexaferrite structure was however be detected in the APS-3 and APS-5 coatings. APS-4 also contains a minor amount of hexaferrite. The APS-3 and APS-5 coatings were both sprayed using a feedstock having the coarsest particle size distribution (Table 3); moreover, the APS-3 coating was deposited using a larger flow rate of primary plasma gas (Ar), and the APS-5 one was sprayed with lower H2 flowrate. The APS-4 coating was sprayed using a finer feedstock, but the arc current was lower than in all other cases. All of these parameter settings are consistently directed toward the minimization of the powder heating, which is likely to cause the presence of some un-melted material in the sprayed coating.

SEM micrographs suggest that the coatings mainly consist of well-flattened lamellae (some of which are indicated by circles in Figure 7), produced from the impact and subsequent solidification of droplets originated by the complete melting of the original agglomerates: the cooling rate experienced by these molten agglomerates upon impact is typically N106 K/s [12] (impact quenching).

Coupling this observation with the previous considerations on the absence of crystalline hexa-ferrite in impact-quenched lamellae, it may be inferred that the hexaferrite peaks found in the above-listed APS coatings reflect the embedment of some un-melted material in them. Nonetheless, the low intensity of the hexaferrite peaks indicates that the differences among the various coatings are not very large, which is also confirmed by the similarity between their microstructures, revealed by SEM micrographs (Figure 8).

The magnetic characteristics of these coatings are, therefore, unsatisfactory: of the first series of APS coatings, the highest saturation magnetization values were produced by coatings APS-3, 4 and 5, in accordance to the presence of some hexaferrite phase, but those values (Table 3) are still much inferior to those of pure crystalline $BaCoTiFe_{10}O_{19}$ because the fraction of the magnetic phase is still too low.

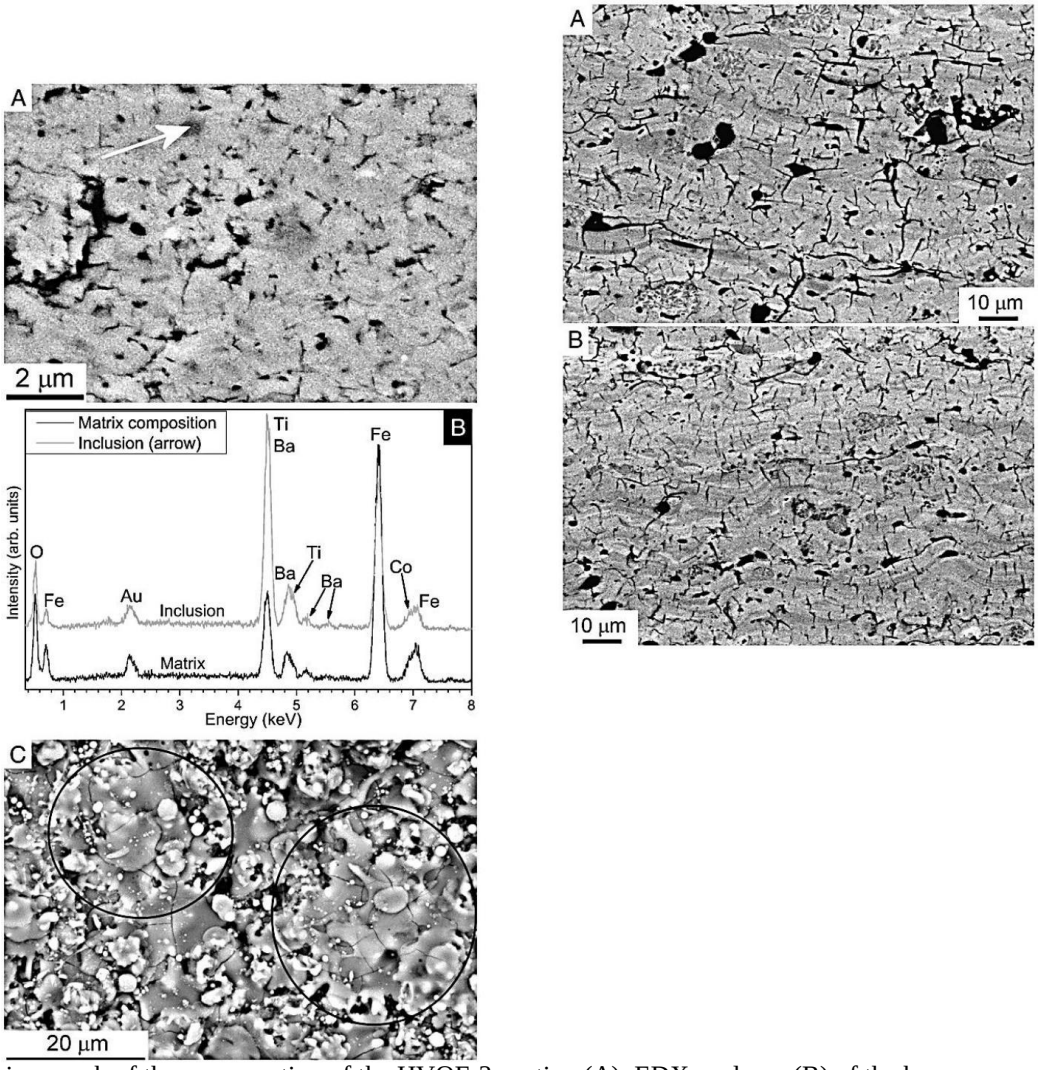

Figure 7: SEM micrograph of the cross-section of the HVOF-3 coating (A); EDX analyses (B) of the homogeneous matrix and of the dark inclusion indicated by an arrow in panel A; SEM micrograph of the surface of the HVOF-3 coating (C).

The magnetic characteristics of these coatings are, therefore, unsatisfactory: of the first series of APS coatings, the highest saturation magnetization values were produced by coatings APS-3, 4 and 5, in accordance to the presence of some hexaferrite phase, but those values (Table 3) are still much inferior to those of pure crystalline $BaCoTiFe_{10}O_{19}$ because the fraction of the magnetic phase is still too low.

The analysis of the HVOF coatings and of the first series of APS coatings provided some important indications. The $BaCoTiFe_{10}O_{19}$ agglomerates which are completely molten in the gas jet cannot produce lamellae having the hexaferrite structure, because of impact quenching. The most straightforward way to preserve the hexaferrite phase would therefore seem to retain a controlled amount of unmelted material. In the HVOF-sprayed coatings, this could not be achieved, whatever the flame stoichiometry. The HVOF process also has limited flexibility for further adjustments; the use of a coarser particle size distribution would probably cause difficulties during spraying, and, even if some unmelted particles would reach the substrate, they would presumably rebound because of their very high velocity. Using the APS technique, by contrast, some unmelted material could be retained: its amount in the APS-1 to APS-6 coatings is too low, but, thanks to the flexibility of the plasma-spraying process, the deposition parameters can be modified for minimal agglomerate melting.

The APS-7 coating (Table 3) was therefore sprayed using the coarser particle size distribution, and spray parameters included low arc current, high Ar flow rate and no H_2 addition, in order to increase the plasma velocity and to minimize its enthalpy andthermal conductivity. This coating actually contains lots of unmelted agglomerates, where the individual micrometric particles are still clearly recognizable, but it is definitely too thin and defective to have some technological interest (Figure 9A). Probably, under these deposition conditions, too many agglomerates were completely unmelted, so that most of them rebounded off the substrate, unacceptably impairing the deposition efficiency. Because of such very large defectiveness and inhomogeneity, the magnetic properties of this coating are still unsatisfactory (Table 3). In order to overcome this trouble while preserving a sufficient number of unmelted agglomerates, the APS-8 coating was sprayed using a different powder feedstock, whose particle size distribution was enlarged (Table 2), so that some finer spray-dried granules can melt and act as a "glue", conferring better cohesion to the abundant unmelted material. Accordingly, this coating is thicker and more homogeneous than APS-7 (Figure 9B): dense regions entrain numerous unmelted agglomerates, which are clearly seen both on polished sections (Figure 9B, circles) and on fractured sections (Figure 9C, circle). Detailed views of the fractured section also reveal that, inside these agglomerates, some of the micron-sized particles acquired a rounded shape (Figure 9D, arrow) and started to form necks (Figure 9D, circles). APS-8 coating contains a major amount of crystalline Ba-hexaferrite due to which this coating provides very satisfactory magnetic properties. It is suggested that this coating can be very promising for electromagnetic wave absorption applications. The ratio between the operating bandwidth and the thickness of a quarter-wavelength-thick absorbing layer deposited onto a reflecting metal plate, has an upper bound which linearly depends on the static magnetic permeability of the layer itself [13].

APS-8 coating contains a major amount of crystalline Ba-hexaferrite due to which this coating provides very satisfactory magnetic properties. It is suggested that this coating can be very promising for electromagnetic wave absorption applications. The ratio between the operating bandwidth and the thickness of a quarter-wavelength-thick absorbing layer deposited onto a reflecting metal plate, has an upper bound which linearly depends on the static magnetic permeability of the layer itself [13]. For the APS- 8 coating, μS=1.5; this value is definitely consistent with the previously-mentioned low frequency real permeability of the bulk material, which suggests that the calculated reflection curves in Figure 10 can actually be applied to the plasma- sprayed coating.

Figure 9: SEM micrographs of the APS-7 and APS-8 coatings. (A) APS-7, cross-section; (B) APS-8, cross-section: the circles indicate some unmelted agglomerates; (C) APS-8, fracture surface (secondary electrons): the circle indicates an unmelted agglomerate; label 1 indicates a flattened lamella; label 2 indicates rounded, partially re-solidified material; (D) APS-8, fracture surface: detail of an unmelted agglomerate; the arrow indicates a rounded micrometric particle, the circles indicate areas where neck formation occurred between micrometric particles.

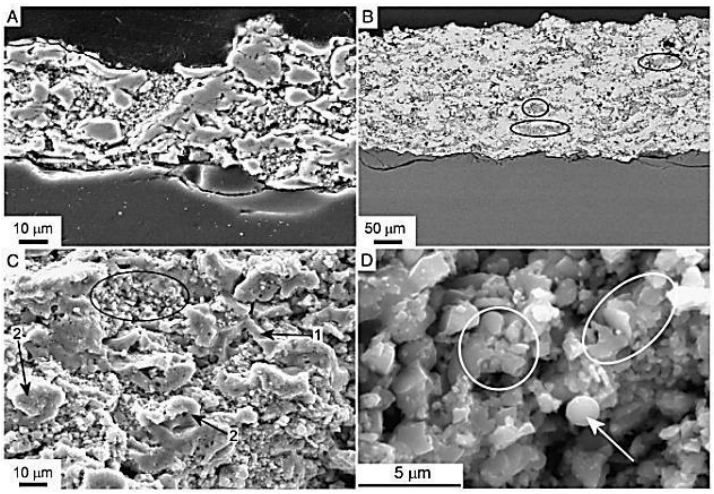

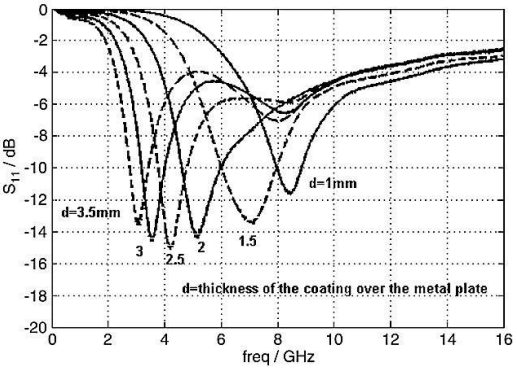

Figure 10: Calculated reflection from a BaCoTiFe10O19-coated metal plate versus coating thickness

It is being concluded that the viability of thermal spraying techniques (particularly of APS) for the production of $BaCoTiFe_{10}O_{19}$ hexaferrite layers, suitable for microwave absorption applications, and provided important information on the relationships between processing conditions, coating structure and resulting magnetic properties. Upon impact on the substrate, molten $BaCoTiFe_{10}O_{19}$ agglomerates cannot produce the crystalline hexaferrite phase, because its crystallization kinetics is too slow in comparison to the very fast cooling rate of impact-

quenched molten droplets. Consequently, intermediate/metastable phases (a spinel crystalline phase and a glassy phase) are formed and the resulting coating does not have the desired magnetic properties. In order to retain the crystalline hexaferrite phase, a controlled amount of unmelted agglomerates should therefore be embedded in the coating. This could not be done by HVOF-spraying, whereas, using the more flexible APS technique, a coating having excellent magnetic properties, close to those of pure crystalline $BaCoTiFe_{10}O_{19}$, could be deposited by devising a suitable set of spray parameters. In this coating, some denser regions, produced by the impact of molten droplets (some of which might have started to re-solidify in-flight), entrain many unmelted agglomerates, where the hexaferrite phase was preserved.

Darja Lisjak et al. had prepared Composite coatings from different volume ratios of hexaferrite ($BaFe_{12}O_{19}$ or $SrFe_{12}O_{19}$) and polyethylene, for the first time, with flame spraying. The hexaferrites –

$BaFe_{12}O_{19}$ (Ba-HF) or $SrFe_{12}O_{19}$ (Sr-HF) – and polyethylene (PE), as a polymer, were mixed and

flame-sprayed onto glass substrates. Most of the thermal energy was consumed for the heating and melting of the polymer and the hexaferrite retained its crystalline structure, while the coatings showed the expected magnetic properties. This system can also serve as a prototype for thermally sprayed composite coatings, which combine a material with high dielectric losses (e.g., a polymer) and one with high magnetic losses (e.g., a ferrite) in order to achieve broadband electromagnetic absorption over a very wide frequency range.

The feedstock powder was prepared from a homogenized stoichiometric mixture of $BaCO_3$ or $SrCO_3$ and Fe_2O_3. Figure 11 shows the X-ray diffractogram of the as-sprayed coating Ba1/3. All the peaks correspond to the hexaferrite structure and were indexed accordingly. A small hump observed at

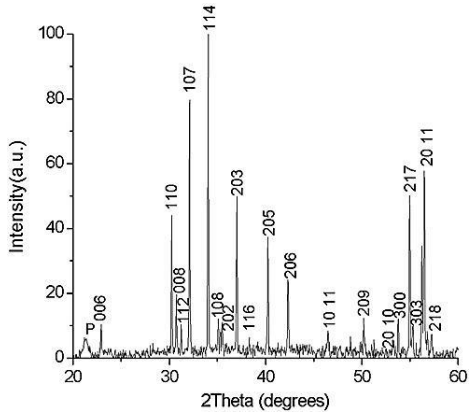

Figure 11: X-ray diffractogram of the Ba1/3 coating: P denotes PE and the indices correspond to the P63/mmc (194) space group.

2Theta ~20–22° originates from the PE. Similar diffractograms were also observed for the other coatings, suggesting that the hexaferrite crystal structure was preserved during the flame spraying in the case of both compositions, Ba- and Sr-HF. Furthermore, the SEM analysis revealed that the hexaferrite agglomerates (bright spherical inclusions in Figure (12A–B) did not melt during the flame spraying.

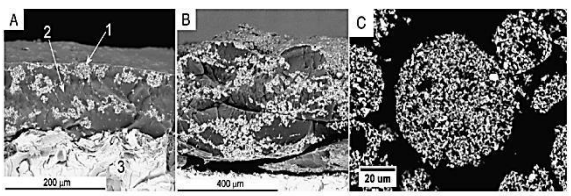

Figure 12: Secondary-electron micrographs of the fracture surfaces of the coatings Sr1/3 (A) and Sr2/3 (B) and backscattered-electron micrograph of the cross-section of the as-sintered hexaferrite feedstock powder (C). Label 1=unmelted hexaferrite particles; label 2=PE matrix; and label 3=substrate.

Their microstructures and sizes remained the same as in the feedstock powder (Figure 12C). Raman spectroscopy confirmed that the non-melted agglomerates retained their original, hexaferrite structure. This confirms that the hexaferrite structure (Figure 11) originates from the preserved feedstock agglomerates. The reflection-loss spectra (Figure 13) calculated from the electromagnetic data. An increased reflection loss (i.e., absorption of 80%) can be observed below 50 GHz for the Ba2/3 coating and above 50 GHz for the Sr2/3 coating (absorption of 65%).

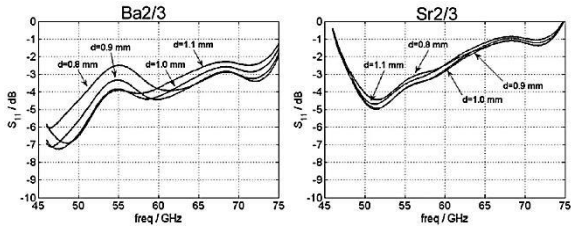

Figure 13: The reflection-loss spectra of the Ba2/3 (left-hand side) and Sr2/3 (right-hand side) coatings

In general, the Ba2/3 coating shows stronger absorption across the whole frequency range studied. The absorption of the Ba1/3 and Sr1/3 was much poorer due to the lower hexaferrite volume ratio than those of the Ba2/3 and Sr2/3. It was being concluded that flame spraying is a very interesting method for the preparation of ceramic/polymer coatings for electromagnetic absorbers.

2. CONCLUSION

Metallic cooper, aluminum and steel as well as non-metallic substrates glass has been used for investigation of coating properties of APS, HVOF & Flame Spraying. Metallic substrates were most commonly explored whereas to investigate magnetic properties of the coatings glass substrate was preferred because of its non-magnetic characteristics. To enhance coating adhesion substrates were degreased using acetone and were grit blasted prior to coating and sometimes bond coat were also required. It has been shown that the microwave absorption strongly influenced by optimum coating thickness and coating angle which were about 100 µm, 500 and respectively. The absorption parameters were also hooked on composition of spraying powders used for different coating techniques. By analyzing SEM & XRD images of all the three types of thermal spraying techniques coatings, a very useful outcome obtained that APS & HVOF spraying techniques unable to retain the crystalline structure of their corresponding powder composites due to high temperature operation envolved; results in poor electromagnetic absorption. On the other hand Flame spraying yields similar results for powder as well as coated samples microstructure & Raman spectroscopy concluded that flame spraying is a very interesting and cost effective method for the preparation of ceramic/polymer coatings for electromagnetic absorbers.

3. REFERENCES

[1] http://www.eccosorb.com/683be594-bcb2-404c-a440-0804f968a82f/download.html.
[2] Z. Yang, F. Luo, W. Zhou, D. Zhu, and Z. Huang, "Design of a broadband electromagnetic absorbers based on TiO2/Al2O3ceramic coatings with metamaterial surfaces," J. Alloys Compd., vol. 687, pp. 384–388, 2016.
[3] S.-E. Lee, J.-H. Kang, C.-G. Kim, Fabrication and design of multi-layered radar absorbing structures of MWNT-filled glass/epoxy plain-weave composites, Compos. Struct. 76 (2006) 397e405.
[4] B. Belaabed, J.L. Wojkiewicz, S. Lamouri, N. El Kamchi, T. Lasri, Synthesis and characterization of hybrid conducting composites based on polyaniline/ magnetite fillers with improved microwave absorption properties, J. Alloys Compd. 527 (2012) 137e144.
[5] P. Saini, V. Choudhary, B. Singh, R. Mathur, S. Dhawan, Enhanced microwave absorption behavior of polyaniline-CNT/polystyrene blend in 12.4e18.0 GHz range, Synth. Met. 161 (2011) 1522e1526.
[6] D. Micheli, C. Apollo, R. Pastore, R.B. Morles, S. Laurenzi, M. Marchetti, Nanostructured composite materials for electromagnetic interference shielding applications, Acta Astronaut. 69 (2011) 747e757.
[7] A.M. Gama, M.C. Rezende, C.C. Dantas, Dependence of microwave absorption properties on ferrite volume fraction in MnZn ferrite/rubber radar absorbing materials, J.Magn. Mater. 323 (2011) 2782e2785.
[8] V.K. Singh, A. Shukla, M.K. Patra, L. Saini, R.K. Jani, S.R. Vadera, N. Kumar, Microwave absorbing properties of a thermally reduced graphene oxide/ nitrile.
[9] V.K Floristán, M., Müller, P., Gebhardt, A., Killinger, A. Gadow, R., Cardella, A., … Kasparek, W. (2011). Development and testing of 140GHz absorber coatings for the water baffle of W7-X cryopumps. Fusion Engineering and Design, 86(9–11), 1847–1850.
[10] D. Lisjak et al., "Preparation of barium hexaferrite coatings using atmospheric plasma spraying," vol. 29, pp. 2333–2341, 2009.
[11] M. Bégard et al., "Surface & Coatings Technology Thermal spraying of Co , Ti-substituted Ba-hexaferrite coatings for electromagnetic wave absorption applications," Surf. Coat. Technol., vol. 203, no. 20–21, pp. 3312–3319, 2009.
[12] P. Fauchais, M. Fukumoto, A. Vardelle, and M. Vardelle, "Knowledge Concerning Splat Formation: An Invited Review," J. Therm. Spray Technol., vol. 13, no. 3, pp. 337– 360, 2004.
[13] K.N. Rozanov, "Ultimate Thickness to Bandwidth Ratio of Radar Absorbers," vol. 48, no. 8, pp. 1230–1234, 2000.